Dynamic Behavior of Suspension Bridges under Moving Loads

Toshiro HAYASHIKAWA* Noboru WATANABE*

(Received June 30, 1982)

Abstract

The dynamic response of suspension bridges subjected to moving loads with a constant velocity is studied. The free vibration analysis of suspension bridges is based on the linearized deflection theory which restricts the amplitudes of vibration to be small, and the dynamic response analysis is conducted by the method of modal analysis. Numerical examples in which actual suspension bridges are used are presented as verification of the analysis. Primary information for an impact factor in suspension bridges is also suggested in this paper.

1. Introduction

In recent years, a new project with respect to long-span suspension bridges is being planned with consideration to the geographical characteristics of Japan. The dynamic behavior of such long-span bridges has become a vitally important engineering problem, because a full understanding of the dynamic characteristics of suspension bridges under various dynamic loads such as wind forces, earthquakes, and moving vehicles is necessary in order to improve their safety margin.

Although the analysis of free vibration of suspension bridges has been investigated by many specialists,[1-5] there are almost no publications dealing with the dynamic response analysis of suspension bridges subjected to moving loads.

To the writers' knowledge, only three investigations[6-9] dealing with such dynamic responses of suspension bridges have been published. Klöppel and Lie[6] calculated the dynamic deflections of a three-span suspension bridge by using a Fourier series solution, but their mode of thinking in modal analysis seems doubtful. The dynamic analysis of a single-span suspension bridge under a moving constant force or a moving pulsating force was investigated by Vellozzi.[7] In the late 1960's, Hirai and Ito[8,9] studied theoretically and experimentally the practicability of railway suspension bridges. They showed that the impact factor is sufficient to discuss about 15% for long-span railway suspension bridges.

The primary objective of this study is to determine a sufficient number of natural frequencies and mode shapes to make possible an accurate dynamic response analysis for practical purposes. The problem is analyzed by the linearized deflection theory, and the effect of restraint conditions of the stiffening girders and the effect of deformations of the

*Department of Civil Engineering, Faculty of Engineering, Hokkaido University, Nishi 8 Kita 13 Kita-Ku, Sapporo, 060, Japan.

tower are considered. The secondary objectives are to obtain a closed form solution for the dynamic response of multispan suspension bridges traversed by moving loads with constant velocity, and to investigate their dynamic characteristics. An approximate calculation formula for the impact factor in suspension bridges is also provided in this paper.

2. Analysis

2-1. Assumptions

In the dynamic response analysis of suspension bridges, conventional assumptions based on the deflection theory are made.[2,3,7] Additional assumptions in the present analysis are as follows:

(1) The amplitudes of vibration are sufficiently small so that the additional horizontal component H_p of the cable tension due to inertia forces is small in comparison with the initial horizontal component H_w of the cable tension due to dead load. This assumption permits the analysis to be based on a linear differential equation.

(2) The types of stiffening girders are grouped into two classes according to their characteristics. The hinged-span type bridge is simply supported at the intermediate supports as shown in Fig. 1(a), and the continuous-span type bridge is continuously supported over all spans as shown in Fig. 1(b).

(3) The boundary conditions of the cable support at the top of the tower are assumed to be as follows: First, the horizontal component of the cable tension H_p is assumed to be the same on both sides of the tower in all spans of the cable (roller connection) as shown in Fig. 2(a). This presupposes that the tower cable saddles are free to move horizontally and there is no tower resistance to the displacement at the top. Second, the horizontal component of the cable tension on both sides of the tower may differ slightly from the friction forces at the tower-cable saddles. This means that the horizontal movement of the tower top is accompanied by a horizontal component of the force between the cable and the tower. Figures 2(b) and 2(c) show the cases of neglecting and considering the effect of an axial force N_i due to the dead load at the tower top, respectively.

(4) In the dynamic response analysis of suspension bridges under moving loads, the

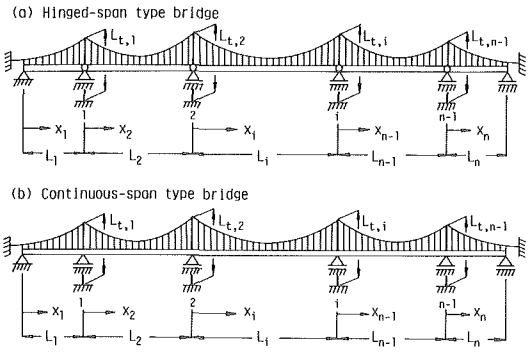

Fig. 1. Geometry and coordinate system of multispan suspension bridges with different types of stiffening girder.

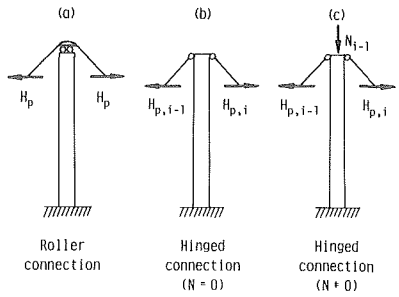

Fig. 2. Boundary conditions of cable support at top of tower.

effects of the damping force and the mass associated with the moving loads are assumed to be negligibly small.

(5) A constant concentrated load P moves from left to right on the multispan suspension bridge with a constant velocity v. At time $t=0$, the moving load arrives at the end of the first span and the dynamic response of the bridge starts at that time from rest condition.

2-2. Free Vibrations

The linearized differential equation for the free vertical vibration of suspension bridges is given[2,3]

$$EI\frac{d^4V(x)}{dx^4}-H_w\frac{d^2V(x)}{dx^2}+\frac{w}{H_w}H_p=\frac{w}{g}\omega^2V(x) \tag{1}$$

in which $V(x)$ is the transverse deflection at the distance x from the left support of the stiffening girder (eigenfunction or mode shape), EI is the flexural stiffness of the stiffening girder, w is the dead load of the bridge per unit length, g is the acceleration due to gravity, and ω is the natural circular frequency. The general solution of Eq. (1) may be expressed in the form

$$V_i(x_i)=A_i\cos\frac{\mu_i x_i}{L_i}+B_i\sin\frac{\mu_i x_i}{L_i}+C_i\cosh\frac{\nu_i x_i}{L_i}+D_i\sinh\frac{\nu_i x_i}{L_i}+\frac{g}{\omega^2H_w}H_{p,i} \tag{2a}$$

in which

$$\mu_i=\sqrt{\frac{H_wL_i^2}{2EI_i}(Z_i-1)},\quad \nu_i=\sqrt{\frac{H_wL_i^2}{2EI_i}(Z_i+1)},\quad Z_i=\sqrt{1+\frac{4w_iEI_i}{gH_w^2}\omega^2} \tag{2b}$$

where the quantity with suffix i indicates that for ith span, and the integration constants A_i, B_i, C_i, and D_i are determined by the boundary conditions of the vibrating structure. The boundary conditions at the left end ($x_1=0$) and the right end ($x_n=L_n$) of the stiffening girder of a multispan suspension bridge are given

$$V_1(0)=0,\quad EI_1\frac{d^2V_1(0)}{dx_1^2}=0,\qquad \text{for } x_1=0 \tag{3a}$$

$$V_n(L_n)=0,\quad EI_n\frac{d^2V_n(L_n)}{dx_n^2}=0,\qquad \text{for } x_n=L_n \tag{3b}$$

The boundary conditions at the intermediate support of the stiffening girder are given as follows:

(1) Hinged-span type bridge as shown in Fig. 1(a)

$$V_{i-1}(L_{i-1})=0,\quad EI_{i-1}\frac{d^2V_{i-1}(L_{i-1})}{dx_{i-1}^2}=0,\quad V_i(0)=0,\quad EI_i\frac{d^2V_i(0)}{dx_i^2}=0 \tag{3c}$$

(2) Continuous-span type bridge as shown in Fig. 1(b)

$$V_{i-1}(L_{i-1})=0,\quad \frac{dV_{i-1}(L_{i-1})}{dx_{i-1}}=\frac{dV_i(0)}{dx_i},\quad V_i(0)=0,\quad EI_{i-1}\frac{d^2V_{i-1}(L_{i-1})}{dx_{i-1}^2}=EI_i\frac{d^2V_i(0)}{dx_i^2} \tag{3d}$$

The following matrix notation may be obtained by substituting Eq. (2a) into Eqs. (3)

$$\boldsymbol{A}\boldsymbol{a}=\boldsymbol{H}\boldsymbol{h} \tag{4a}$$

in which

$$\begin{aligned}&\boldsymbol{a}=\{A_1, B_1, C_1, D_1, A_2, B_2, C_2, D_2, \cdots, A_n, B_n, C_n, D_n\}^T,\\ &\boldsymbol{h}=\{H_{p,1}, H_{p,2}, \cdots, H_{p,n}\}^T\end{aligned} \tag{4b}$$

The orders of the coefficient matrices $\boldsymbol{A}$ and $\boldsymbol{H}$ are $4n\times 4n$ and $4n\times n$ (or $4n\times 1$), respectively. The vector $\boldsymbol{a}$ is of the order $4n\times 1$, while the vector $\boldsymbol{h}$ is either of the order $n\times 1$ in the case of the hinged connection or of the order 1×1 (H_p) in the case of the roller connection.

The remaining unknown quantities $H_{p,i}$ or H_p in Eq. (2a) are related to the eigenfunctions $V_i(x_i)$ by the so-called cable equation. The different connection types of the cable support at the tower top are considered very carefully in the cable equation which relates the elastic streching of the cable to geometric displacement. The equation is as follows:

(1) Roller connection type as shown in Fig. 2(a)

$$\frac{L_c}{E_c A_c}H_p-\frac{w}{H_w}\int_0^L V(x)\mathrm{d}x=0 \tag{5}$$

in which E_c is the modulus of elasticity of the cable, A_c is the cross-sectional area of the cable, and L_c is the virtual length defined by the integral $\int_0^L(\mathrm{d}s/\mathrm{d}x)^3\mathrm{d}x$, in which $\mathrm{d}s$ is a differential element along the cable curve.

(2) Hinged connection type as shown in Figs. 2(b) and 2(c)

$$\frac{L_{c,i}}{E_c A_c}H_{p,i}-\frac{w_i}{H_w}\int_0^{L_i}V_i(x_i)\mathrm{d}x_i=-\delta_i^l+\delta_i^r,\quad \text{for } i=1,2,\cdots,n \tag{6a}$$

in which δ_i^l and δ_i^r are the horizontal displacements of the tower top at the left and right support of the ith span, respectively. In the case where the effect of the axial force is neglected, these displacements can be expressed by

$$\delta_i^l=-\frac{L_{t,i-1}^3}{3E_t I_{t,i-1}}(H_{p,i-1}-H_{p,i}),\quad \delta_i^r=-\frac{L_{t,i}^3}{3E_t I_{t,i}}(H_{p,i}-H_{p,i+1}) \tag{6b}$$

in which $E_tI_{t,i}$ and $L_{t,i}$ are the average flexural stiffness and height of the ith tower, respectively. In the case where the effect of the axial force N_i is considered

$$\begin{aligned}\delta_i^l&=-\frac{L_{t,i-1}}{N_{i-1}}\left[\frac{\tan(K_{i-1}L_{t,i-1})}{K_{i-1}L_{t,i-1}}-1\right](H_{p,i-1}-H_{p,i}),\\ \delta_i^r&=-\frac{L_{t,i}}{N_i}\left[\frac{\tan(K_iL_{t,i})}{K_iL_{t,i}}-1\right](H_{p,i}-H_{p,i+1})\end{aligned} \tag{6c}$$

in which $K_i=\sqrt{N_i/(E_tI_{t,i})}$. The relation matrix equation between the vectors $\boldsymbol{a}$ and $\boldsymbol{h}$ can also be obtained by substituting Eq. (2a) into Eqs. (5) or (6a)

$$\boldsymbol{G}\boldsymbol{a}=\boldsymbol{E}\boldsymbol{h} \tag{7}$$

in which the coefficient matrices $\boldsymbol{G}$ and $\boldsymbol{E}$ are of the orders $n\times 4n$ and $n\times n$ in the case of the hinged connection, and $1\times 4n$ and 1×1 in the case of the roller connection, respectively.

A set of homogeneous equations with the vector $\boldsymbol{a}$ is obtained by eliminating the vector $\boldsymbol{h}$ from Eqs. (4a) and (7)

$$(\boldsymbol{A}-\boldsymbol{H}\boldsymbol{E}^{-1}\boldsymbol{G})\boldsymbol{a}=\boldsymbol{0} \tag{8}$$

For non-trivial solutions $\boldsymbol{a}$ it is required that the determinant of the coefficient matrix of Eq. (8) should vanish

$$\det|\boldsymbol{A}-\boldsymbol{H}\boldsymbol{E}^{-1}\boldsymbol{G}|=0 \tag{9}$$

This Eq. (9) is a frequency equation of multispan suspension bridges and is a transcendental equation on the natural circular frequencies ω. The roots are obtained by applying the Regula-Falsi method[10] and by using a high-speed digital computer. The relative values of elements in the vectors $\boldsymbol{a}$ and $\boldsymbol{h}$ corresponding to a particular value of natural circular frequency can be obtained by Eqs. (8) and (7), respectively. Furthermore, the eigenfunction $V_i(x_i)$ of Eq. (2a) which is also called the modal shape function is determined by replacing the corresponding natural circular frequency.

2-3. Forced Vibrations

The modal analysis method is used to determine the dynamic response of suspension bridges subjected to moving loads. The dynamic deflection function $\eta(x,t)$ is expressed as simply as possible mathematically

$$\eta(x,\ t)=\sum_{m=1}^{\infty} V_m(x)\,q_m(t) \tag{10}$$

in which $q_m(t)$ is the time function. The Lagrange's equation leads to the following equation of motion for elastic structures

$$\ddot{q}_m(t)+\omega_m^2 q_m(t)=\frac{Q_m(t)}{\frac{w}{g}M_m^2} \tag{11a}$$

in which a dot denotes the differentiation with respect to time t, $Q_m(t)$ is the general force, and

$$M_m^2=\int_0^L V_m^2(x)\mathrm{d}x=\sum_{i=1}^{n}\int_0^{L_i} V_{mi}^2(x_i)\mathrm{d}x_i \tag{11b}$$

The term of external force $Q_m(t)$ in Eq. (11a) is determined from the series expansion of loads (see Ref. 11), and is formulated in the case of a concentrated load P with a constant velocity v

$$Q_m(t)=P\cdot V_m(vt) \tag{12}$$

The solution of Eq. (11a) is obtained by using the Laplace transform method as follows:

$$\eta(x_r,\ t_s)=\sum_{m=1}^{\infty} V_{mr}(x_r)[\Phi_{ms}(t_s)+\Psi_{ms}(t_s)] \tag{13a}$$

in which

$$\Phi_{ms}(t_s)=\frac{P}{\frac{w_s}{g}\omega_m M_m^2}\int_0^{t_s} V_{ms}(v\tau)\sin[\omega_m(t_s-\tau)]\mathrm{d}\tau,$$

$$\Psi_{ms}(t_s)=q_{ms}(0)\cos\omega_m t_s+\frac{\dot{q}_{ms}(0)}{\omega_m}\sin\omega_m t_s \tag{13b}$$

where the constants $q_{ms}(0)$ and $\dot{q}_{ms}(0)$ are determined from initial conditions at the time $t_s=0$, and the subscripts r and s present the measuring and loading span number of multispan suspension bridges, respectively. When the moving load traverses the second span and subsequent spans, the constants $q_{ms}(0)$ and $\dot{q}_{ms}(0)$ are obtained by the following equations

$$q_{ms}(0)=\Phi_{m,s-1}\left(\frac{L_{s-1}}{v}\right)+\Psi_{m,s-1}\left(\frac{L_{s-1}}{v}\right),\quad \dot{q}_{ms}(0)=\dot{\Phi}_{m,s-1}\left(\frac{L_{s-1}}{v}\right)+\dot{\Psi}_{m,s-1}\left(\frac{L_{s-1}}{v}\right),$$
$$\text{for}\quad s=2,3,\cdots,n \tag{14}$$

The dynamic deflection of multispan suspension bridges at any point can be computed by Eq. (13a). Furthermore, the slope and the bending moment of suspension bridges can be obtained by the first and the second derivatives of Eq. (13a) with respect to the space coordinate x, respectively.

3. Numerical Examples

Numerical examples are presented to demonstrate the effectiveness of the analysis and to show some characteristics of the dynamic behavior of suspension bridges. The prototypical examples are three kinds of three-span suspension bridges having center span lengths of 315, 770, and 1100 m. Their geometries and structural properties, necessary for the dynamic analysis, are summarized in Table 1.

3-1. Natural Frequencies

The computed natural periods of A, B, and C bridges are presented for the first five modes of the asymmetric and symmetric vibration in Tables 2, 3, and 4, respectively. It is seen from these tables that there is a slight difference in the lower modes of symmetric vibration, between the roller connection and the hinged connection. On the other hand, the difference due to cable supports at the top of the tower is not recognized in the higher modes of vibrations. Also, there is a considerable difference between the hinged-span type and the continuous-span type bridges. The values of the natural periods of suspension

TABLE 1. Characteristics of sampled suspension bridges (1t=9.81kN).

Characteristic values		A bridge	B bridge	C bridge
Stiffening girder	L_2 (m)	315	770	1100
	L_1 (m)	85	250	260
	w_2 (t/m)	8.12	10.155	10.485
	w_1 (t/m)	8.12	10.545	10.785
	I_2 (m^4)	0.6	2.452	5.591
	I_1 (m^4)	0.6	2.108	5.877
	E_s (t/m^2)	2.1×10^7	2.1×10^7	2.1×10^7
Cable	f_2 (m)	35	76	100
	A_c (m^2)	0.0901	0.2280	0.3853
	E_c (t/m^2)	1.6×10^7	2.0×10^7	2.0×10^7
Tower	L_t (m)	60.000	138.850	180.257
	I_t (m^4)	1.000	3.320	10.466
	E_t (t/m^2)	2.1×10^7	2.1×10^7	2.1×10^7

TABLE 2. Computed natural periods (in seconds) of vertical vibration of A bridge.

Mode types of vertical vibration	Mode order	Hinged-span type			Continuous-span type		
		Roller connection	Hinged connection (N = 0)	Hinged connection (N ≠ 0)	Roller connection	Hinged connection (N = 0)	Hinged connection (N ≠ 0)
Asymmetric mode	1st	3.2262	3.2262	3.2262	2.7121	2.7112	2.7113
	2nd	1.0912	1.0881	1.0884	1.0057	1.0044	1.0045
	3rd	0.9463	0.9463	0.9463	0.7488	0.7484	0.7485
	4th	0.4360	0.4360	0.4360	0.4058	0.4058	0.4058
	5th	0.2486	0.2486	0.2486	0.2679	0.2679	0.2679
Symmetric mode	1st	2.6846	2.6267	2.6282	2.6792	2.6189	2.6205
	2nd	1.5650	1.5619	1.5620	1.4668	1.4652	1.4654
	3rd	1.0319	1.0283	1.0283	0.8473	0.8458	0.8458
	4th	0.6190	0.6189	0.6189	0.5492	0.5491	0.5491
	5th	0.3229	0.3229	0.3229	0.3133	0.3133	0.3133

TABLE 3. Computed natural periods (in seconds) of vertical vibration of B bridge.

Mode types of vertical vibration	Mode order	Hinged-span type			Continuous-span type		
		Roller connection	Hinged connection (N = 0)	Hinged connection (N ≠ 0)	Roller connection	Hinged connection (N = 0)	Hinged connection (N ≠ 0)
Asymmetric mode	1st	6.7851	6.7851	6.7851	6.2628	6.2608	6.2619
	2nd	3.9884	3.9742	3.9821	3.4933	3.4849	3.4896
	3rd	2.5489	2.5489	2.5489	2.3190	2.3189	2.3190
	4th	1.2935	1.2935	1.2935	1.3094	1.3094	1.3094
	5th	0.7696	0.7696	0.7696	1.1180	1.1180	1.1180
Symmetric mode	1st	5.9576	5.9357	5.9479	5.6374	5.6179	5.6287
	2nd	3.9424	3.9405	3.9416	3.8749	3.8734	3.8742
	3rd	2.7698	2.7697	2.7698	2.5621	2.5620	2.5620
	4th	1.7620	1.7620	1.7620	1.6596	1.6596	1.6596
	5th	0.9819	0.9819	0.9819	1.2037	1.2037	1.2037

TABLE 4. Computed natural periods (in seconds) of vertical vibration of C bridge.

Mode types of vertical vibration	Mode order	Hinged span type			Continuous-span type		
		Roller connection	Hinged connection (N = 0)	Hinged connection (N ≠ 0)	Roller connection	Hinged connection (N = 0)	Hinged connection (N ≠ 0)
Asymmetric mode	1st	8.1045	8.1045	8.1045	7.4380	7.4376	7.4377
	2nd	3.2200	3.2200	3.2200	3.1490	3.1481	3.1485
	3rd	2.9623	2.9591	2.9605	2.4451	2.4438	2.4444
	4th	1.6896	1.6896	1.6896	1.5704	1.5704	1.5704
	5th	1.0236	1.0236	1.0236	0.9980	0.9980	0.9980
Symmetric mode	1st	5.9345	5.9046	5.9068	5.6621	5.6233	5.6253
	2nd	4.4255	4.4115	4.4128	4.3643	4.3554	4.3566
	3rd	2.6686	2.6615	2.6617	2.5115	2.5085	2.5087
	4th	2.2635	2.2629	2.2629	1.9869	1.9856	1.9856
	5th	1.2957	1.2957	1.2957	1.2296	1.2295	1.2295

bridges with hinged stiffening girders are generally large in comparison with those of suspension bridges with continuous stiffening girders.

The effect of the vibration in the flexural stiffness of towers upon the natural frequencies is given in the following. Figure 3 shows the relation between the flexural stiffness ratio of the tower to the stiffening girder of center span and the first natural period for the symmetric mode of vibrations of the B bridge. When the flexural stiffness of the tower

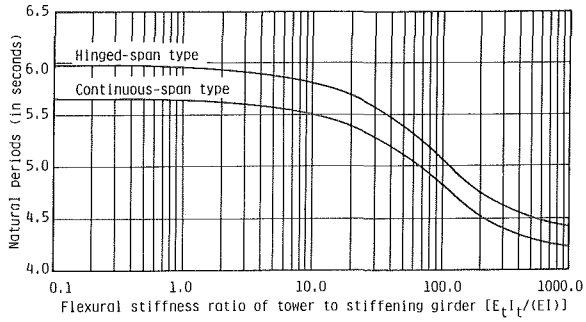

Fig. 3. Effect of flexural stiffness of tower upon natural periods of free vertical vibration of B bridge.

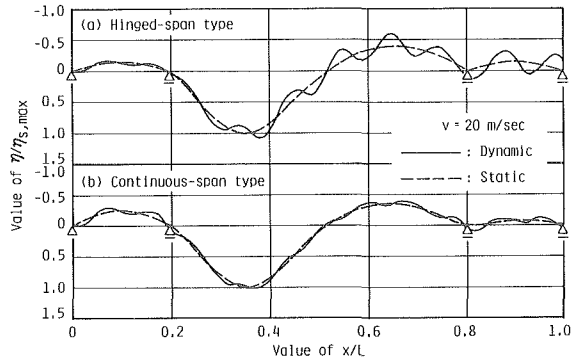

Fig. 4. History curves of deflection at quarter point of second span ($L_2/4$).

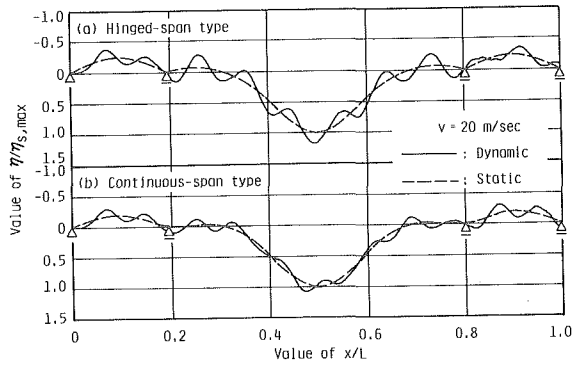

Fig. 5. History curves of deflection at center point of second span ($L_2/2$).

decreases, the natural period gradually approaches that of the roller connection (hinged-span type = 5.9576 sec ; and continuous-span type = 5.6374 sec). It can be concluded that the effect of the flexural stiffness of the tower can be known only when the value of $E_tI_t/(EI)$ is approximately larger than 10. In other words, the difference due to cable supports at the tower top arises when the flexural stiffness of the tower increases by about 10 times that of the stiffening girder. From a practical point of view, however, the deformation of the tower may be neglected in the analysis of free vertical vibrations, because the range of values of $E_tI_t/(EI)$ is approximately from one to five.

3-2. Response History Curves

In Figs. 4 and 5 are shown the response history curves of deflection for the B bridge when a concentrated load with a constant velocity $v=20$ m/sec is passing through from left to right. The abscissa in these figures represents the distance between the left support and the position of the load on the bridge normalized with respect to the total bridge length. The ordinate of the history curves presented herein is normalized with respect to the maximum static response value of the measuring points under consideration. Also shown in broken lines in each figure is the static response, that is the response if the speed of the moving load approaches zero.

Although numerical computations are carried out using up to 12 terms of the series of Eq. (13a), there is no significant difference between the roller connection and the hinged connection in the numerical results. The static responses at the quarter point and the center point of the second span seem to be governed almost entirely by the fundamental mode of asymmetric and symmetric vibrations as shown in Figs. 4 and 5, respectively.

It is also clear that the static response of the hinged-span type bridge produces the bent-angle (discontinuous slope form) at the intermediate supports. On the other hand, there is no bent-angle in the static response of the continuous-span type bridge as shown in Figs. 4(b) and 5(b). This fact suggests that continuous suspension bridges offer more advantages for railway vehicles running through them than hinged suspension bridges.

The dynamic amplification factor δ defined by the following equation[11] is used to evaluate dynamic effects (the term dynamic effects is used herein to denote the difference between the dynamic response and the static response)

$$\delta=\frac{\eta_{d,max}-\eta_{s,max}}{\eta_{s,max}}\times 100\ (\%) \tag{15}$$

in which $\eta_{d,max}$ and $\eta_{s,max}$ are the maximum values of the dynamic and static response, respectively. It is seen from Figs. 4(a), 4(b), 5(a), and 5(b) that the dynamic amplification factors calculated by Eq. (15) are 8.70%, 2.48%, 18.40%, and 2.72%, respectively.

3-3. Effect of Speed

The effect of speed is described by the speed parameter α.[9,11] This parameter is a nondimensional quantity which depends on the load speed, flexural stiffness, mass per unit length, cable sag length, and span length of suspension bridges. The relation between the dynamic amplification factor of deflection and the speed parameter is shown in Figs. 6, 7, and 8. The δ-α relation diagrams for the range of values of the speed parameter $0.0\leqq\alpha\leqq$

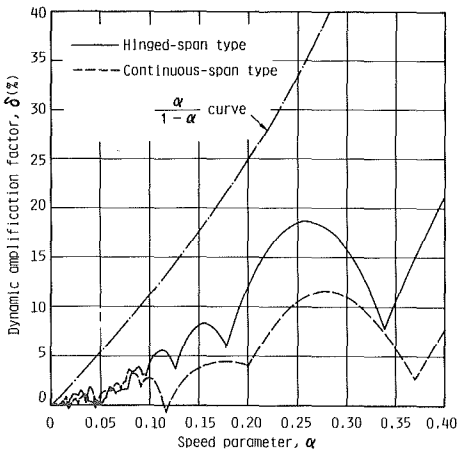

Fig. 6. δ-α relation diagram for deflection at center point of first span ($L_1/2$) of A bridge.

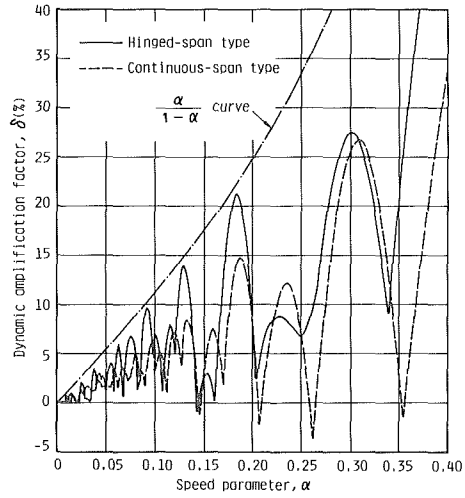

Fig. 7. δ-α relation diagram for deflection at center point of second span ($L_2/2$) of B bridge.

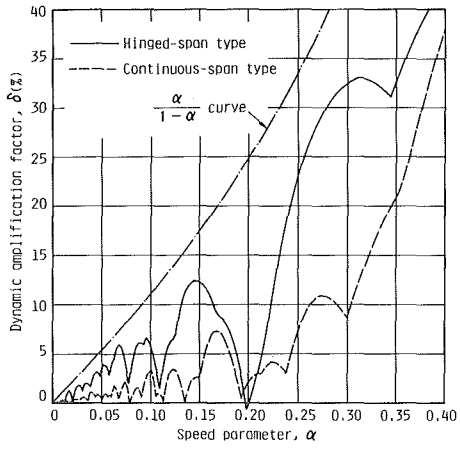

Fig. 8. δ-α relation diagram for deflection at quarter point of second span ($L_2/4$) of C bridge.

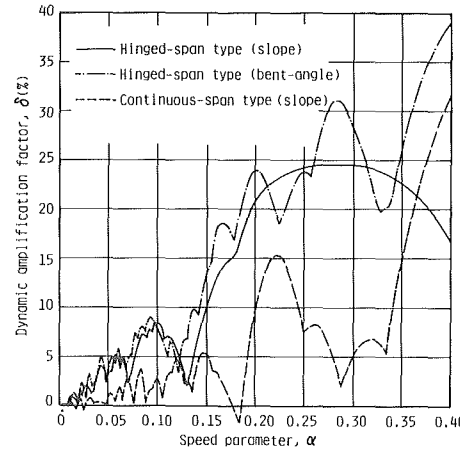

Fig. 9. δ-α relation diagram for slope and bent-angle at first intermediate support ($x_2=0$) of A bridge.

0.40 is calculated by increasing in increments of 0.0025. It is seen in these figures that the dynamic amplification factors have a number of local peaks and possess a general tendency to increase as the speed parameter increases.

Also, the dynamic amplification factors of the hinged suspension bridges are very large in comparison with those of the continuous suspension bridges. The maximum deflection of a suspension bridge occurs frequently in the neighborhood of the quarter point of the center span. A significant difference between the hinged-span type and the continuous-span type bridges is observed in the δ-α relation diagrams for deflection at this point ($L_2/4$). Furthermore, the dynamic amplification factor at $L_1/2$ and $L_2/2$ is about the same or less

than that at $L_2/4$. The supplemental curves $\alpha/(1-\alpha)$[9] shown in these figures represent such properties as the enveloping line of the dynamic amplification factors.

The relation between the dynamic amplification factor and the speed parameter for slope and bent-angle at the first intermediate support ($x_2=0$) is shown in Fig. 9. In the same manner as the deflections described above, the dynamic amplification factors for the slope of the hinged suspension bridge are very large in comparison with those of the continuous suspension bridge. Although the continuous suspension bridge by no means produces the bent-angle at the intermediate supports, the hinged suspension bridge produces the bent-angle.

It is also worth noticing that the dynamic amplification factor of the bent-angle is of considerable dimensions.

3-4. Impact Factor

The dynamic amplification factor discussed in this paper corresponds to the impact factor in bridge design. The estimation of impact factor is a complicated planning problem, because the impact is influenced by various factors[9] such as the effects of moving mass, wave propagation, hammer-blow force of wheel and vehicle-springs. The impact factor specification is not at present considered for highway bridges having a span length of more than 200 m. However, it is presumed from the above-mentioned consideration that the impact factor must be included to a certain degree in the bridge design of stiffening girders. From the computed results of three kinds of bridges shown in Table 1 and other suspension bridges with the various span lengths, the impact factor i_η in suspension bridges may be calculated by the following equations

$$i_\eta = \frac{220}{400+\ell} \text{ , for the hinged-span type bridge} \tag{16a}$$

$$i_\eta = \frac{120}{300+\ell} \text{ , for the continuous-span type bridge} \tag{16b}$$

in which ℓ is the span length of suspension bridges. The above formulae will give a close approximation to the required value within the limitation of moving speed from 100 km/hr to 150 km/hr.

The effect of uniformly distributed loads is neglected in this study, but it is possible to consider the effect in the calculations. However, the impact factor for a distributed load may be considered less than that for a concentrated moving load. The effect of structural damping is also neglected in the above investigation, but it can be estimated from the damping characteristics expected in an actual bridge that the dynamic effects will decrease by several percent.[11] It should be noted that the value calculated from Eqs. (16) makes a rough estimation of the impact factor and is slightly large. When one uses them practically, an overestimation for the impact factor in long-span suspension bridges gives a safe-side design consideration.

4. Conclusions

In this study a procedure for the dynamic response analysis of multispan suspension

bridges subjected to moving loads has been developed. Since the solution is expressed in a closed form, the dynamic response at any time and at any point on the bridge can be easily obtained. Also, the final form of the solution is simple and very convenient for making a computer program of suspension bridges.

It can be concluded from the numerical results of natural frequencies that the effect due to the difference in the cable support conditions at the tower top is negligibly small in suspension bridges. However, the effect due to the difference in the support conditions of the stiffening girder is considerable.

The values of the natural periods of hinged suspension bridges are generally larger than those of continuous suspension bridges. The dynamic effects produced by moving loads generally increase with decreasing span length and increasing speed of moving loads. The dynamic effects of hinged suspension bridges are very large in comparison with those of continuous suspension bridges. Also, hinged suspension bridges produce the bent-angle at the intermediate supports and their dynamic amplification factors indicate large values. Finally, it is concluded from an engineering standpoint that the continuous-span type of suspension bridges has the advantage of good stability for railway vehicles in comparison with the hinged-span type normally used in suspension bridges.

Acknowledgments

The writers wish to thank Mr. H. Ohshima of the Honshu-Shikoku Bridge Authority for his providing of technical data on suspension bridges. The numerical computations were carried out with the digital computer HITAC M-200H of the Hokkaido University Computing Center, and work on numerical examples was greatly assisted by the continued efforts of Mr. K. Hashiba who was a graduate student of the Hokkaido University (an engineer of the Ministry of Construction at present). The writers gratefully acknowledge the financial support from the Scientific Research Fund (Bounty Research A) of the Ministry of Education granted to one of the writers.

References

1) Abdel-Ghaffar, A. M.: Proc. of ASCE, **106** (1980), ST10, pp. 2053-2075.
2) Bleich, F. et al.: Dept. of Commerce, Bureau of Public Roads, U. S. Gov. (1950).
3) Maeda, Y. et al.: Proc. of JSCE, (1977), 262, pp. 13-24.
4) Moppert, H.: Statische und dynamische Berechnung erdverankerter Hängebrücken mit Hilfe von Greenschen Funktionen und Integralgleichungen, (1955), Stahlbau-Verlages-GmbH, pp. 58-114.
5) Steinman, D. B.: J. of the Franklin Institute, **268** (1959), 3, pp. 148-174.
6) Klöppel, K. and Lie, K. H.: Ingenieur-Archiv, **13** (1942), 5, pp. 211-266.
7) Vellozzi, J.: Proc. of ASCE, **93** (1967), ST4, pp. 123-138.
8) Hirai, A. and Ito, M.: Proc. Int. Symp. on Susp. Bridges, (1966), pp. 285-291.
9) Ito, M.: Proc. of JSCE, (1968), 149, pp. 1-17.
10) Wendroff, B.: Theoretical Numerical Analysis, (1966), Academic Press.
11) Hayashikawa, T. and Watanabe, N.: Proc. of ASCE, **107** (1981), EM1, pp. 229-246.